Proceedings, 7th African Rift Geothermal Conference
Kigali, Rwanda 31st October – 2nd November 2018

Geophysical Imaging of the Luhoi Geothermal Field, Tanzania

Egidio Armadillo[1], Daniele Rizzello[2], Claudio Pasqua[3], Taramaeli Mnjokava[4], Jonas Mwano[4], Makoye Didas[4], Lucas Tumbu[4]

[1]DISTAV, Universita' di Genova, Italy. [2]Tellus s.a.s., Italy. [1-3]ELC-Electroconsult, Italy. [4]Tanzania Geothermal Development Company Ltd (TGDC), Tanzania

egidio@dipteris.unige.it; rizzello@tellus-explora.eu; claudio.pasqua@elc-electroconsult.com; taramaeli.mnjokava@tanesco.co.tz; jonas.mwano@tanesco.co.tz; makoye.didas@tanesco.co.tz; lucas.tumbu@tanesco.co.tz

Keywords:

Luhoi, magnetotellurics, gravity, modelling

ABSTRACT

The Luhoi prospect is a coastal basin located within Rufiji Trough along the passive continental margin of western Indian Ocean of Tanzania, a sector extending south of the termination of the eastern branch of the African Rift System. The structural pattern is dominated by tectonic features belonging to the WNW-ESE Tagalala Trend and to the NE-SW Selous Trend that have been active until recent times. The thermal manifestations are mostly located along the WNW-ESE flowing the Ruhoi River, in the south-western sector of the focal area. The Wingoyongo Hill, located in the north-eastern sector of the focal area, forms a morphological high where emissions of H2S and bituminous staining were observed. Here an old well intersected 800 m of quartz sandstone with minor intercalations of siltstone and claystone (Kipatimu Series, Lower Cretaceous). Magnetotelluric (MT), time-domain electromagnetic (TDEM) and gravimetric geophysical surveys were carried as part of a geoscientific study funded by the Ministry of Foreign Affairs of Iceland through Icelandic International Development Agency (ICEIDA) and the Nordic Development Fund (NDF). The survey area extends over a surface of approximately 75 km^2, designed to include the Luhoi hot springs and the Wingoyongo fumaroles. The gravimetric data set is composed of 124 measurements collected on a regular grid at a nominal spatial sampling of 800 m, and 16 more to infer the regional field. The residual Bouguer anomaly map shows an elongated gravimetric high trending NE-SW with values up to 3 mGal, surrounded by gravimetric lows up to -2 mGal. Forward and inverse 2D/3D models image an asymmetrical horst like structure trending NE-SW. Both the thermal manifestations and the Wingoyongo Hill are aligned along the NW flank of the horst. Since the Wingoyongo well intersected sandstones for about 800 m, the horst like structure is interpreted as made by the Kipatimu sandstones. The two depressions bordering the horst like structure are filled with lower density materials, likely siltstones, claystones and/or mudstones, with an estimated maximum thickness of 1.1 km. The MT and TDEM data were acquired at 76 locations, with a nominal spatial sampling of 750 m. The static shift effect has been corrected by TDEM/MT phases joint inversion. MT impedances and tippers have been estimated by means of the remote reference technique with robust processing methods coupled with a coherence rejection

scheme. Resistivity 3D inversion reveals two conductive anomalies coincident with the low-density sedimentary rocks bordering the horst structure. A clear updoming of resistivity marks the NW flank of the horst and it is interpreted as due to a combined effect of different alteration, lithology and fluid content and to reflect the main upflow of the geothermal system.

1. Introduction

With the aim to assess its geothermal potential, the Luhoi prospect has been recently covered by a multidisciplinary geophysical survey. The site is located within the Tanzania Coastal Basin, at about 120 km southwest of the town of Dar es Salaam (Fig.1).

Magnetotelluric (MT), Time Domain Electromagnetic (TDEM) and gravity surveys were carried out between January 24 and March 12, 2017, by TGDC (Tanzania Geothermal Development Company), and Tellus (Italy) under the supervision of ELC-Electroconsult (Italy). The campaign was accomplished during two consecutive phases. The second phase was conceived to get the more detail as possible where the first one indicated greater geological variations.

The work was funded by the Icelandic International Development Agency (ICEIDA) and the Nordic Development Fund (NDF), with the aim to support geothermal exploration and capacity building in East Africa.

The Tanzanian Coastal Basin has been object of petroleum exploration since the 50's, with about 35 wells (Kent, 1971) widespread across it, among which a relatively shallow borehole is located in the north-eastern sector of the focal area.

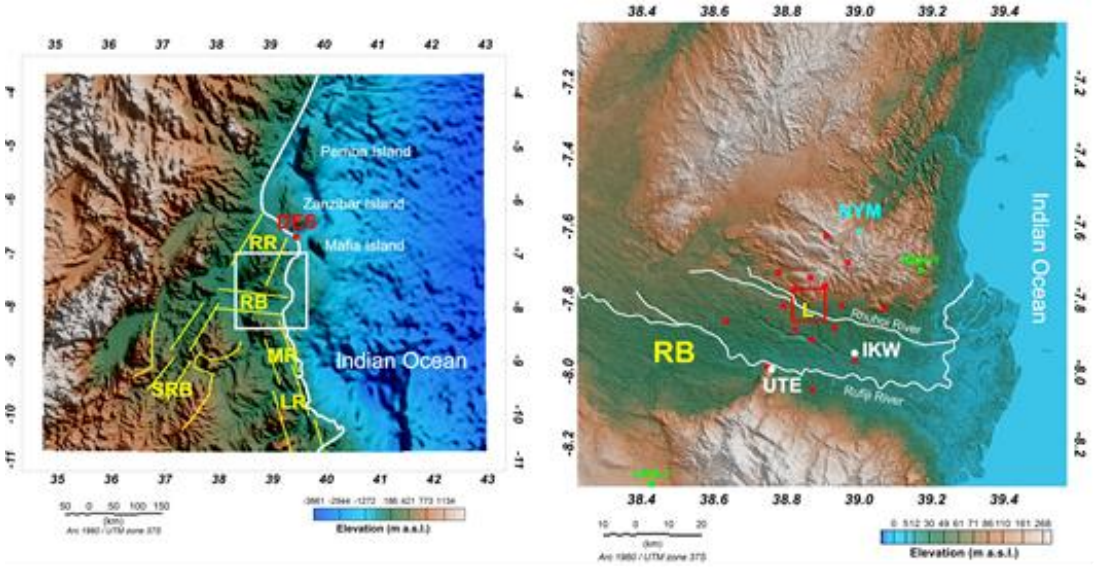

Figure 1: Location of the Luhoi survey area. L: Luhoi area (marked by a red rectangle); RB: Rufiji Basin; RR: Ruvu Rift; SRB: Selous Rift Basin; LR: Lindi Rift; MR: Mandawa Rift. Town and villages of Dar Es Salaam, Ikwiriri and Utete are marked by "DES", "IKW" and "UTE", respectively. The MT reference site (Nyambili) is labelled "NYM". The wells are marked as RKN-1 (Ruaruke North-1) and LKO-1 (Lukuliro-1). Main rivers are marked by white lines.

2. Geological Setting

The Luhoi prospect is located on the northern limit of the Rufiji trough, a tectonic depression with WNW/SSE trend lying within the southeast Tanzanian Coastal Basin. This basin can be considered as part of the southeastern branch of the EARS (Chorowitz, 2005), and is

constituted by two sub-basins: the NNW-SSE Mandawa rift basin and NE-SW Selous rift basin (Fig.1). The Neoproterozoic Pan African metamorphic basement complex (Balduzzi *et al.* 1992) is outcropping between the two. In particular, the Luhoi prospect is located a few kilometers north of the intersection between the two tectonic trends, just close to the northern limit of the Rufiji tectonic basin (Fig.1). In the Coastal Basin, a thick sequence of clastic and limestone products was deposited starting from the Jurassic on top of the Karoo sequence and of the basement complex. The thickness of this sedimentary sequence has been estimated between 4,000 and 6,000 m, and it's the results of several transgressions/regression phases occurred from Middle Jurassic to Cenozoic (Kapilima, 2003).

The geological section of the survey area (ELC, 2017a) is displayed in Figure 3. The oldest formation outcropping in the area are the Lower Cretaceous Kipatimu sandstones (with a thickness of 1,000-1,800 m), overlain by the Lower Cretaceous Limestones. The Kipatimu sandstones are covered by the Quaternary Conglomerate, lateritic soil and Alluvial and colluvial deposits, with a thickness not exceeding a few tens of meters.

The overall stratigraphy in the Luhoi prospect has been estimated by integration of data arising from wells drilled for oil exploration and the geological survey accomplished. The well location is shown in Fig.1, while the inferred geological section is displayed in Figure 3, together with the well stratigraphy.

The Ruaruke North-1 well (TD 2,000 m), located at 35 km ENE from the area, penetrated Upper Cretaceous Claystones interbedded with siltstone, shale and sandstone deposited in marine facies. From 1,180 m to bottom, the Lower Cretaceous/Upper Jurassic sandstones belonging to the Kipatimu formation were found. The Lukuliro-1 (TD 2,367 m), located at 78 km SSW intersected down to 927 m the Kipatimu sandstones, below which Upper to Middle Jurassic limestones were found down to 2,181 m. From this depth down to the bottom hole, the Permian to Triassic Karoo Sandstones were penetrated. The Wingoyongo-1 well was drilled to 762 m in the Wingoyongo Hill, located in the eastern portion of the survey area, close to an outcrop of Kipatimu Sandstones (Fig.2). The well intersected quarzitic sandstone with some mineralization and bituminous staining. Anomalous thermal conditions are reported, starting from 64 m up to the well bottom, as well as low-T alteration minerals down to about 100 m. Furthermore, as reported by Kent (1971), immediately E and W of the Wingoyongo well, two shallow boreholes penetrated the Upper Cretaceous Claystones from the surface down to 60 m depth. However, no surface evidence of this formation was found in the area.

The main structural trends over the area are: the NW to WNW Tagalala Trend, related to the Maminzi - Tagalala Fault Zone crossing the coastal basin of Tanzania in correspondence of the Rufiji basin; the NE to NNE Selous Trend, constituting the western margin of the Tanzania coastal basin, and crossing the study; the N to NNW Lindi Trend, detectable only in the diagram only by remote sensing (ELC, 2017b).

The most important geothermal manifestations in the area are the Luhoi hot springs (ranging from 59.5 to 71.6°C) and the Wingoyongo fumaroles. The estimated reservoir temperature is about 95°C (ELC, 2017c).

3. Geophysical Investigations

The area covered by geophysical investigations was about 67 km^2 (9 x 7.5 km). A comprehensive view of the geophysical station layout is given in Figure 2.

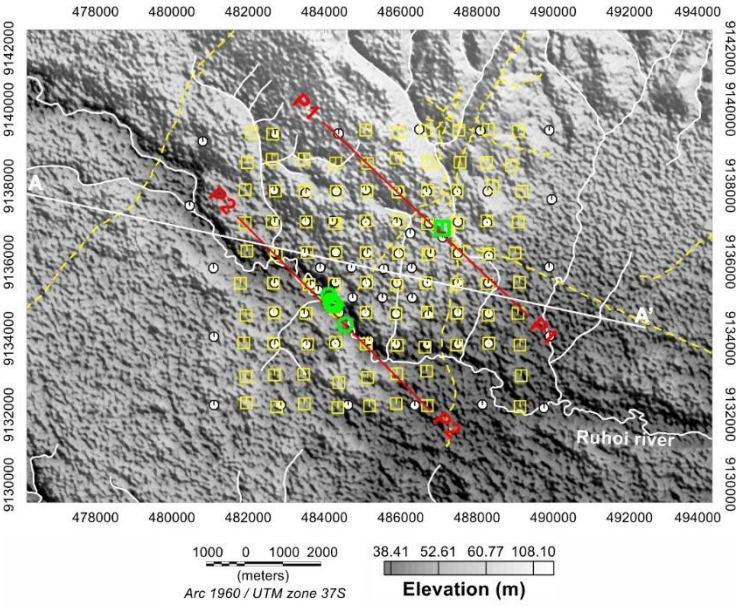

Figure 2: Locations of the geophysical stations (MT/TDEM stations white dots, gravity stations yellow squares). The Luhoi hot springs are marked by green circles for reference, while the Wingoyongo hill fumaroles by a green square. White lines indicate the main rivers, while yellow dashed lines mark the main roads. Profile P1, P2, P3 are marked by red lines. Bottom: geological map of the area.

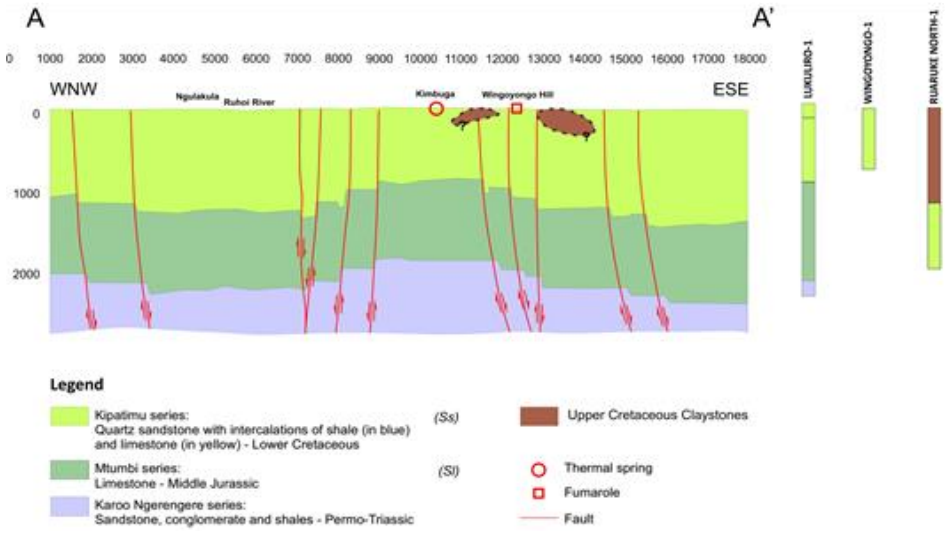

Figure 3: The SW-NE geological section across the Luhoi area (modified from ELC, 2017a). See Figure 2 for its location. The well stratigraphy is also shown (right).

Magnetotelluric (MT) and Time Domain Electro Magnetics (TDEM) measurements were carried out by TGDC personnel over the Luhoi area at 76 stations, with a minimum nominal spacing of 800 m. More detailed sampling was set around the geothermal springs, while nineteen stations were located around the central survey area with a spacing of 1.75 km, in order to better constrain the 3-D inversion.

The gravity survey consists of 124 stations on a detailed grid over the focus area, hundred of which were arranged over a rectangular grid with nominal station inter-spacing of 800 m, with a 60 m tolerance from the ideal position. Other 24 stations were located in the central area to get more detail in that zone. Additionally, 16 sparse stations were located to infer the regional field to compute the residual anomalies. The total number of gravity stations resulted 140.

3.1 Results of the MT and TDEM investigations

Three Phoenix V5 System MT equipments acquired EM data in the 1,000-0.0001 Hz range. One remote reference station was located in Nyambili, about 20 km away from the survey area (Fig.1). Mean record length was of 26.3 hrs. Software developed at the University of Genova was used to estimate the MT impedance and geomagnetic tipper, by combining the remote reference technique (Gamble et al., 1979) and robust MT processing (Sutarno, 2008) with coherence check (Jones and Jodicke, 1984). The resulting impedance and tipper resulted of good quality, thanks to good field practice. The MT static shift was corrected by means of joint inversion of MT phase and TDEM apparent resistivity data, providing the two apparent resistivity correcting factors (s_{xy}, s_{yx}) for each station. Joint inversion was carried out by means of the Meju (1996) approach. The MT impedance was corrected by assuming that the static distortion can be modelled by the following linear relationship,

$$\boldsymbol{Z}_c = \boldsymbol{C}\,\boldsymbol{Z}_d \tag{1}$$

where $\boldsymbol{C}$ is a diagonal matrix which elements are the correcting factors, and $\boldsymbol{Z_d}$ and $\boldsymbol{Z_c}$ are the distorted and corrected impedance, respectively.

While one-dimensional inversion provided a first good approximation of the subsurface resistivity structure, we performed 3-D inversion for interpretation. The inversion has been carried out by means of the ModEM software, a FD software designed for parallel computing (Meqbel, 2009; Egbert and Kelbert, 2012; Kelbert et al., 2014). We used the full (unrotated) and static shift - corrected impedance tensor (Z), jointly with Tz from the whole dataset, using 19 periods in the range between 0.003 s and 1,000 s. We assigned error floors of 5% of $|(Z_{xy} Z_{yx})|^{1/2}$ to the Z_{xy} and Z_{yx} impedance tensor components, and 100 % of $|(Z_{xy} Z_{yx})|^{1/2}$ for Zxx and Zyy. A constant value of 0.05 was used as an error floor for the tipper components. The grid used for the model under consideration consists of 70 x 70 x 95 cells in x – y and z - directions (Fig.4). In the central portion the horizontal cell size is 300 m. At shallow depth, the minimum height of each cell is 25 m. The cell width increases logarithmically towards the edges of the model, and with depth. To take into account the effect of the Indian Ocean on the EM data, it has been included in the model, by using ETOPO1-bathymetry (1 arc-minute resolution), keeping the water resistivity fixed to 0.3 Ohm m. Inversion runs were performed from different initial models to validate the results. Our final run derived from the initial model obtained by the interpolation of 1D models.

The discussion of the model is hereafter developed by resistivity cross-sections and horizontal slices. Two cross-sections (SP1, SP2, Fig.5) are here discussed; their location is shown in Figure 2. We have identified the bottom of the conductive layer by the iso-resistive 10 Ohm m (dotted black line); the inferred faults are marked by white dashed lines; the resistive bedrock is identified by the iso-resistive 50 Ohm m contour line (dotted white line).

The main observations are discussed hereafter:

- The sections are characterized by two conductive layers (0.5-10 Ohm m) that can be separated by a discontinuity D. The NW layer (C1) is shallower and with uniform thickness, the SE one (C2) is deeper and with a thickness increasing toward SE.
- It can be noticed that the manifestations occur near the 10 Ohm m isoresistivity line updoming. Moreover, the highest conductivity is visible close to the Wingoyongo fumaroles. These layers can represent a shallow low-T alteration zone in the Kipatimu sandstones or could be ascribed to the aforementioned Upper Cretaceous Claystones.

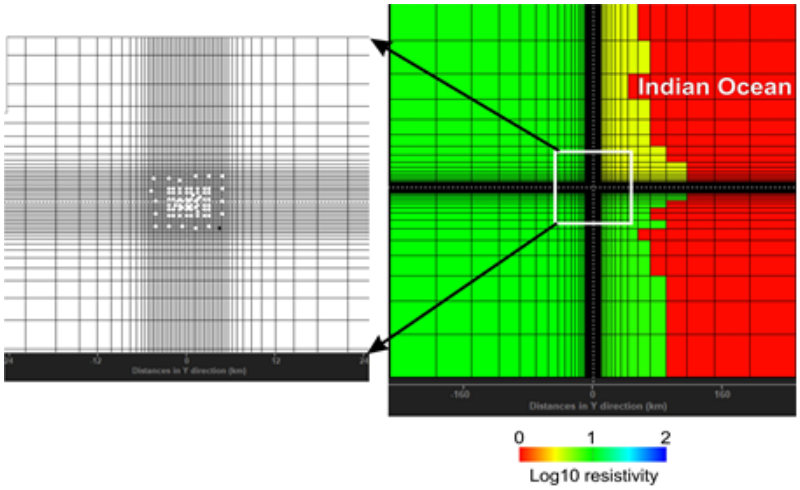

Figure 4: The horizontal grid used. Right: the whole grid, showing the inclusion of Indian Ocean. Left: particular of the grid in the survey area. MT stations are marked by white dots.

The shallow and thin SR layer (15-20 Ohm m) could represent a recent basin alluvial infill or sandstones intercalations in the Claystones.

- The resistivity bedrock identified by the white dashed line is located at about 4-4.5 km depth. Ideally, its top lies inside the Karoo rock series (see Fig.3). No clues about the presence of the Lower Cretaceous Limestones are visible. To verify that this could not be an effect of the 3D smooth inversion, we also performed 1D blocky, obtaining an equivalent result. On the other hand, the thickness of the Kipatimu Sandstones inferred from well Lukuliro-1 (fig.2) is not compatible with the Karoo top depth. We concluded that the Limestones don't provide a sufficient resistivity contrast to be detected by MT.

From the horizontal resistivity slices (Fig.6), it can be observed that:

- C1 develops toward NW, while C2 toward SE. The SR shallow resistive layer described above, is limited to a portion of the SE sector of the area (100 m b.s.l. slice).
  The D discontinuity, retrieved by analyzing several profiles (not shown here) spans the whole survey area and its main direction is NE to NNE, compatible with the Selous Rift trend. This supports the hypothesis of its tectonic origin. Its shape suggests that a N-S trend could be superimposed; the N-S direction is compatible with the Lindi Trend.
- The strong conductivity around the Wingoyongo fumaroles is associated to the D discontinuity, suggesting a tectonic control on geothermal alteration patterns. At the same time the Luhoi hot springs lie at the intersection of the D feature with the NW-SE Tagalala lineaments inferred from remote sensing (thin red lines).
- The NE-SW trend is somehow still visible down to 2,000 m b.s.l. (slice not shown). At greater depths, the average resistivity approaches 50 Ohm m. This background value should be considered as the resistivity of the unaltered Karoo formation (see geological section, Fig.3). However, the analysis of the iso-50 Ohm m surface (not shown) revealed it shows undulations down to 5-6 km b.s.l. depth, compatible with the NE-SW trend;
  this indicates that the Selous Rift tectonics affected the rock basement at great depths.

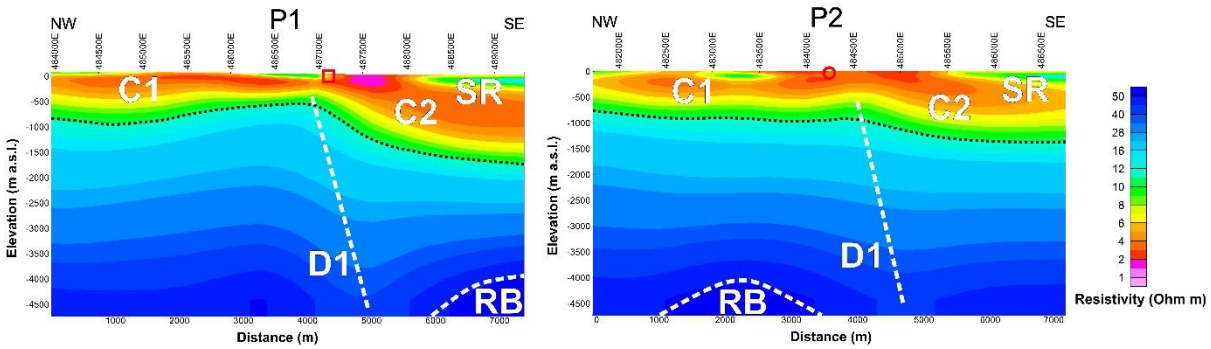

Figure 5: Sections P1 and P2. The red square indicates the location of the Wingoyongo hill manifestations, the red circle the Luhoi hot springs.

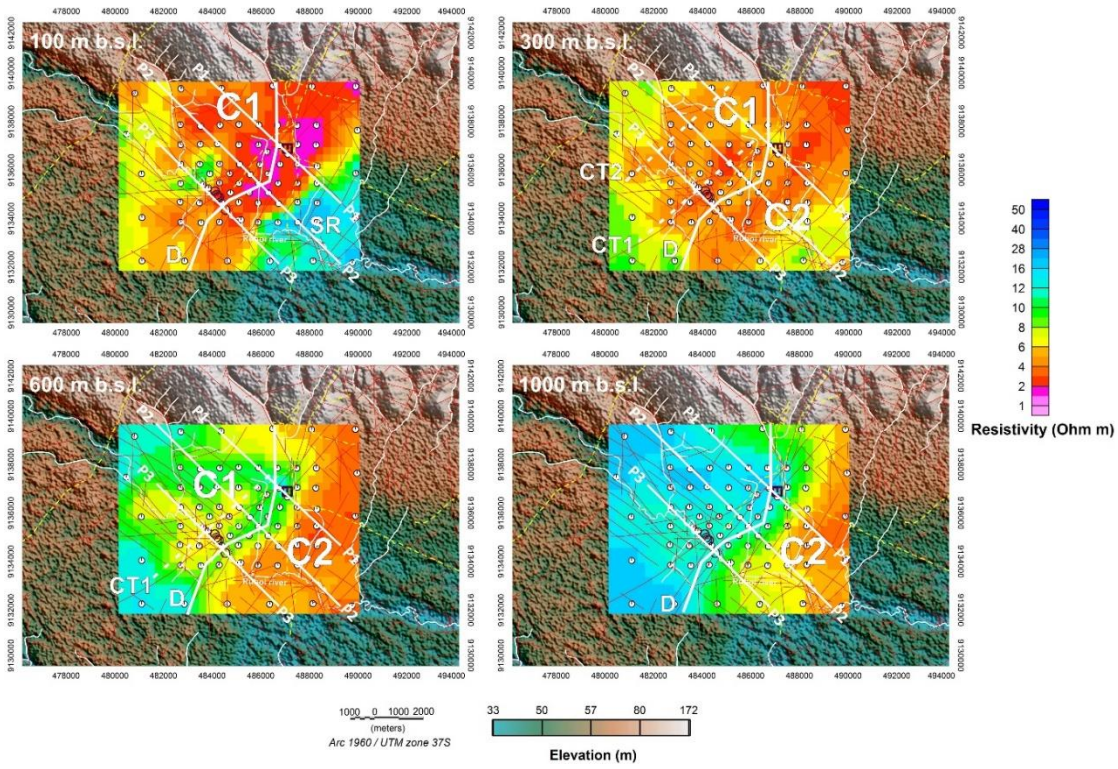

Figure 6: Horizontal slices of the 3D model from 100 m to 600 m b.s.l. White dots: MT stations. Black circles: Luhoi hot springs; black square: Wingoyongo hill manifestations. White line indicates the inferred lineament, white dashed lines the hypothesized lineaments. The main resistivity features are labelled "C1" and "C2". The thin red lines mark the lineaments inferred from remote sensing. White thin lines indicate the main rivers, while yellow lines the main roads.

3.2 The gravity survey

Gravity measurements were carried out by a G927 LaCoste & Romberg meter equipped with electronic beam, levels and feedback system. Data were acquired in combination with differential GPS positioning, which allowed to a vertical precision <0.1 m for most of the stations. Corrections for scale factor, tide, drift, latitude, free air, Bouguer and topography were applied. The mean of the absolute value of the closure errors was 34 microGal, while the estimated measurement error was about 31 microGal.

To estimate the Bouguer density, we first tried to apply the Parasnis approach (Parasnis, 1951), but with no success, may be due to a strong regional field. We then assumed the mean value for the sandstones' densities reported in Daly et al., 1966, that resulted to be 2.40 g/cm^3.

In order to get the residual Bouguer anomaly (BA) map, we have estimated the regional gravimetric field by means of the "regional" stations located around the survey area (see Fig.1). The regional field has been obtained by smoothing the Bouguer anomaly by a 7 km gridding. The pattern of the regional BA and the residual BA map are shown in Figure 6. The residual BA shows an elongated anomaly trending NE-SW. This feature is parallel to some lineations detected by remote sensing (ELC, 2017b), and is compatible with the Selous Rift, also observable at regional scale (Fig.6, left). We can therefore hypothesize that the NE-SW faults defining the structure, belong to a regional system, which can affect the bedrock at great depths.

In order to emphasize the structural lineaments, we have computed the BA horizontal (Fig.8, left). Furthermore, we have estimated the depth of the sources (Fig. 8, right.) via the Spector and Grant (1970) method and the 3D Euler Deconvolution (Reid et al., 1990); the depth range between was 0.5-1 km and was used in the subsequent 2D and 3D modelling.

3.2.1. 2D Modelling

We have performed forward 2D modelling along the profiles shown in the map of Figure 6. The profiles are perpendicular to the main NE-SW anomaly shown in the Residual Bouguer Anomaly map, and therefore the assumption of 2D density distribution is expected to be a good approximation.

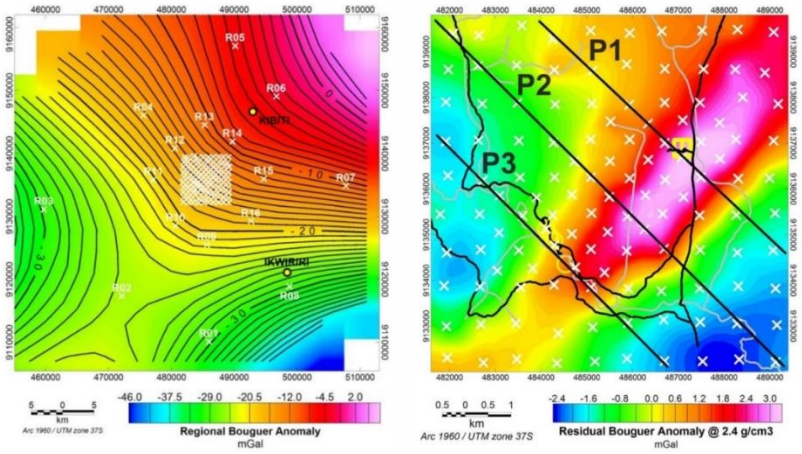

Figure 6: Left: the regional Bouguer anomaly map. The white crosses represent the station locations. Right: Residual Bouguer anomaly map at 2,400 kg/m^3. White crosses: measurement point locations. Yellow circles: thermal manifestations. Yellow square: Wingoyongo hill. Black lines: main roads. Grey lines: main rivers. The gravity profiles are labelled P1, P2, P3.

The main Bouguer anomalies to be modelled are the high anomaly values trending NE-SW and the corresponding low values that border the gravimetric high.

The Wingoyongo well is located at the NW margin of the positive elongated anomaly and drilled about 760 m of sandstones. Therefore, we have assumed that the gravimetric high is linked to the presence of the sandstones, and the gravimetric lows are due to surrounding lighter material.

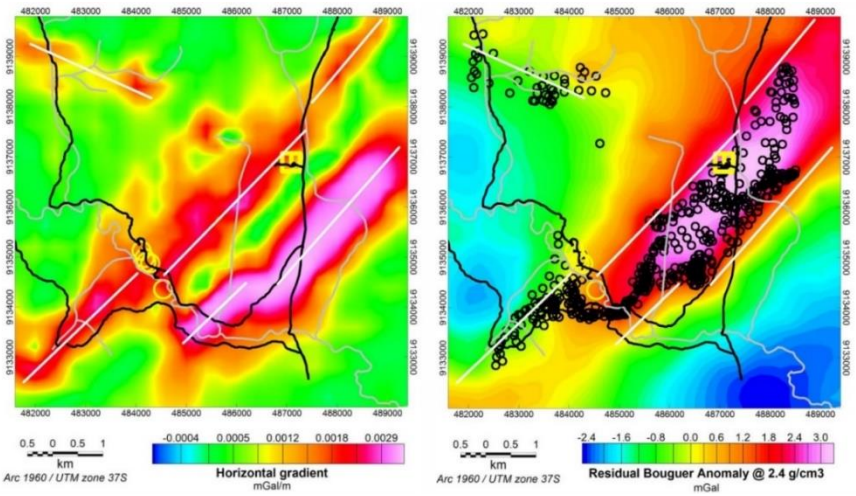

Figure 7: Left: Horizontal gradient of the residual Bouguer anomaly. The white lineaments have been traced following the local maxima. Yellow circles: thermal manifestations. Right: location of the 3D Euler deconvolution solutions (black circles), mapping the horizontal location of the sources. Yellow square: Wingoyongo hill. Black lines: main roads. Grey lines: main rivers.

The sandstones have been given a density of 2,400 kg/m^3 (Daly et al. 1966), while the low-density medium a density of 2,250 kg/m^3; this medium could could be associated with the Upper Cretaceous Claystones, or to alteration affecting the Kipatimu Sandstones at their top.

The modelling has been carried out by means of a two-layer configuration, without taking into account the possible presence of limestones at depth (on the other hand, only hypothesized); finally, the interfaces between high and low-density media are horizontal or close to vertical (>70°), simulating extensive structures.

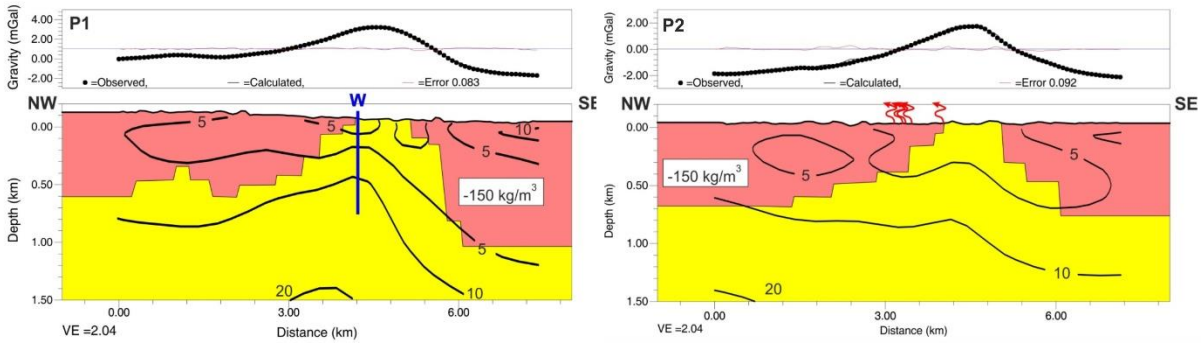

Figure 8: 2D forward modelling of the residual Bouguer anomaly along profile P1, P2, P3. Upper panel: observed gravity (black dots) vs calculated gravity (black continuous line); red line: errors. Lower panel: 2D density model. The contour lines (5, 10, 20 Ohm m) of the 3D MT resistivity model are superimposed on the density model. Yellow: sandstones with reference density 2,400 kg/m^3. Ochre: low density region (2,250 kg/m^3). W: Wingoyongo well.

The 2D models are shown in figure 8. The sections are characterized by a horst-like structure made by denser sandstones reaching the surface, and by shallow lower density materials (-150 kg/m3) extending NW and SE. The horst structure is asymmetric; the interface at the SE side of the horst is steeper and deeper than the one at the NW side.

The resistivity distribution derived from the 3D MT model is superimposed on the models. The resistivity and density patterns are well correlated, since the conductive regions correspond with the lower density regions. Therefore, resistivity seems to be controlled by lithology rather than by alteration mineralogy. Low density regions could then be attributed to the Upper Cretaceous Claystones. However, below the Wingoyongo well, where the correlation is fainter,

hydrothermal alteration probably affects the Kipatimu Sandstones, as also suggested by the Wingoyongo logs. It can be observed that the Wingoyongo fumaroles and the hot springs are located along the NW border of the horst structure.

3.2.2 3D Modelling

With the aim to obtain the topography of the low-high density material interface, we performed a 3D inversion by the GMSYS-3D software package of Oasis Geosoft. A model is defined by a number of stacked surface grids with density specified for the layer below each surface.

Calculations are performed in the wave number domain and are based on the Parker's algorithm (Parker, 1972). The topographic surface is the ASTER DEM, de-sampled at 200 m. Below the surface, we have considered a simple layer with density of -150 kg/m^3, which bottom has been set at an initial depth of -500 m a.s.l. Below this plane, we have assumed the Kipatimu Sandstone at 0 kg/m^3. The bottom of the model has been fixed at -2,000 m a.s.l.

The inverted final density contrast (-150 kg/m^3) surface is shown in Figure 9 as an elevation grid a.s.l.

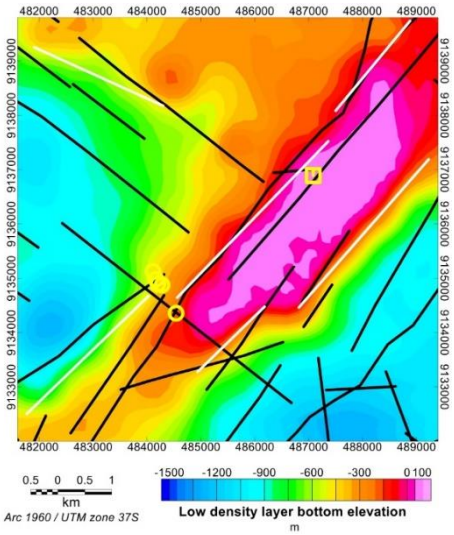

Figure 9: Elevation a.s.l. of the low density (2250 kg/m3) layer bottom. White lines: gravimetric lineaments derived from the analysis of the residual BA horizontal gradient. Black lines: remote sensing lineaments that are likely controlled by the elevation variations of the sandstones top, implying a structural control. Yellow circles: thermal manifestations. Yellow square: Wingoyongo fumaroles.

The map shows the NE-SW horst, culminating between the Wingoyongo fumaroles and the Luhoi hot springs. As already inferred from 2D modelling, the structure is clearly asymmetric, since it is steeper toward SE. In the NW half of the area, it can be seen that the sandstones' top surface progressively lowers toward SW. This lowering appears as a step-descent driven by the NW-SE (normal) faults inferred by remote sensing in that zone (heavy black lines), that can be attributed to the Tagalala Rift tectonics.

4. Conclusions

Geophysical modelling allowed us to improve the geological knowledge of the area. The updated geological section can be observed in Figure10.

The MT and TDEM surveys detected an about 1 km - thick conductive layer. Beneath this layer, the Kipatimu Sandstones were detected, with a resistivity of about 10 Ohm m at their

top. The Upper Cretaceous Limestones were not discerned by MT, although their presence is suggested by the thickness of the sandstones. Bedrock undulations indicate that the NE-SW structure could be present down to 5 - 6 km. An elongated, central NE-SW elongated resistivity updoming was inferred, to which all the manifestations on the area are related. A tectonic control on this structure appeared quite plausible.

Gravity modelling was restricted to 2 km depth, since the geophysical data was well explained by considering the geological structures above. Indirect deep information come from the regional Bouguer Anomaly map suggests that the bedrock is plausibly affected by Selous-trend faults down to great depths, confirming the deep features imaged by MT. An asymmetric, NE-SW elongated horst, culminating between the fumaroles and the hot springs was depicted. This structure reaches the surface nearby the Wingoyongo fumaroles. The horst resulted surrounded by low-density layers, extending toward SE and NW across the whole area.

Magnetotelluric and gravity modelling showed several analogies: the conductive regions have a correspondence with the low-density zones, and the resistivity updoming roughly corresponds with the horst imaged by gravity.

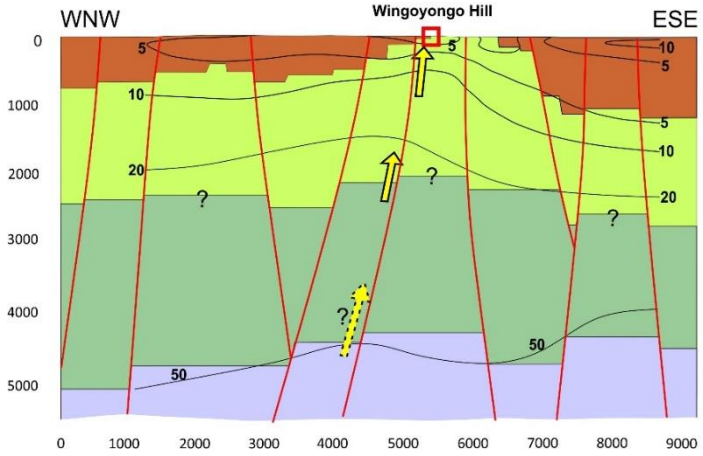

Figure 10: The revised geological section. The direction of the section is the same as the A-A' section, but its length is restricted to the geophysical survey area. Yellow arrows indicate possible fluid paths. Black lines indicate the isoresistivity contour. Refer to Figure 2 for legend.

The conductive-low density zones around the horst has been interpreted as the Upper Cretaceous Claystones; the shallow resistivity signature is then mostly of lithological origin. The resistivity updoming below the Wingoyongo fumaroles is however much less pronounced than the corresponding density high. It is then inferred that geothermal alteration is here an important factor, and plausibly developed down to about 500 m depth.

The deep faults inferred by both the geophysical methods in the area, likely affecting the Karoo formation. Although reservoir depth couldn't be estimated, these structures could act as a preferred path to surface for fluid upraise from great depths.

AKNOWLEDGEMENTS

This work was founded funded by the Icelandic International Development Agency (ICEIDA) and the Nordic Development Fund (NDF). The Tanzania Geothermal Development Company (TGDC), ELC-Electroconsult S.p.A., Tellus s.a.s. and the Department of Earth, Environment and Life Sciences of the University of Genoa (DISTAV) provided instrumental and technical support.

REFERENCES

Balduzzi A, Msaky E, Trincianti E and Manum SB “Mesozoic Karoo and post-Karoo formations in the Kilwa area, southeastern Tanzania - a stratigraphic study based on palynology, micropaleontology and well log data from the Kizimbani Well”. J. Afr. Earth Sci. vol. 15, (1992), 405–427.

Daly R. A., G. Edward Manger, Sydney P. Clark, Jr. DENSITY OF ROCKS. In: Handbook of Physical Constants. Edited by Sydney P. Clark, Jr., GSA Memoirs, Geological Society of America (1966), 97 pp.

Egbert, G.D. & Kelbert, A. "Computational recipes for electromagnetic inverse problems". Geophys. J. Int.,189(1), (2012), 251-267.

ELC Electroconsult (a). "Luhoi Geological Report" (Milan, Italy, unpublished, 2017).

ELC Electroconsult (b). " Luhoi Remote sensing Report" (Milan, Italy unpublished, 2017).

ELC Electroconsult (c), "Luhoi Geochemical Report" (Milan, Italy, unpublished, 2017).

Gamble, T.D., Goubau, W.M., Clarke, J. "Magnetotellurics with a remote magnetic reference". Geophysics, 44, (1979) 53-68.

Kapilima, S. "Tectonic and sedimentary evolution of the coastal basin of Tanzania during the Mesozoic times". Tanz. J. Sci. (2003), Vol 29 (I).

Kelbert A, Meqbel N, Egbert GD, Tandon K. "ModEM: A modular system for inversion of electromagnetic geophysical data". Computers & Geosciences, 66, (2014), 40-53.

Kent, P.E., Hunt, J.A., Johnstone, D.W. "Geology and Geophysics of Coastal of Tanzania". Natural Environment Research Council, Institute of Geological Sciences (1971), pp. 1-101 (Geophysical Paper 6).

Jones A.G.and Jodicke H. “Magnetotelluric transfer function estimation improvement by a coherence-based rejection technique”. Paper presented at 54th Annual International Meeting, Soc. of Expl. Geophys., Atlanta, Ga., Dec. 2-6, 1984.

Meju, M. "Joint inversion of TEM and distorted MT soundings: some effective practical considerations". Geophysics, 61, (1996) pp. 56-65.

Meqbel, N. "The electrical conductivity structure of the Dead Sea Basin derived from 2D and 3D inversion of magnetotelluric data". PhD thesis, Free University of Berlin, Berlin, Germany, (2009).

Parasnis D.S. "A study of rock densities in the English Midlands". Roy. Astr. Soc., Geophys. Suppl., 6, (1951),252-71.

Parker R.L. "The Rapid Calculations of Potential Anomalies". Geophys. J. R. Astr. Soc. 31, (1972), 447-455.

Reid A. B., J. M. Allsop, H. Granser, A. J. Millet and I. W. Somerton. "Magnetic interpretation in three dimensions using Euler deconvolution". Geophysics, VOL. 55, (1990), NO. I, 80-91.

Spector A, and F.S. Grant. "Statistical models for interpreting aeromagnetic data". Geophysics, vol. 35 (1970) no. 2, 293-302Annex 1 – Field Data and Corrected Values.